



Recruitment of host's progenitor cells to sites of human amniotic fluid stem cells implantation

Teodelinda Mirabella^{a,b,1}, Alessandro Poggi^{b,1}, Monica Scaranari^b, Massimo Mogni^c, Mario Lituania^c, Chiara Baldo^c, Ranieri Cancedda^{a,b}, Chiara Gentili^{a,b,*}

^a Department of Oncology, Biology, and Genetics, University of Genova, Largo Rosanna Benzi 10, 16132 Genova, Italy

^b National Cancer Research Institute, Largo Rosana Benzi 10, 16132 Genova, Italy

^c Galliera Hospital, Via A. Volta 6, 16128 Genova, Italy

ARTICLE INFO

Article history:

Received 1 December 2010

Accepted 19 December 2010

Available online 2 April 2011

Keywords:

Mesenchymal stem cells

Tissue engineering

Angiogenesis

Inflammation

In vivo test

In vitro test

ABSTRACT

The amniotic fluid is a new source of multipotent stem cells with a therapeutic potential for human diseases. Cultured at low cell density, human amniotic fluid stem cells (hAFSCs) were still able to generate colony-forming unit-fibroblast (CFU-F) after 60 doublings, thus confirming their staminal nature. Moreover, after extensive *in vitro* cell expansion hAFSCs maintained a stable karyotype. The expression of genes, such as SSEA-4, SOX2 and OCT3/4 was confirmed at early and later culture stage. Also, hAFSCs showed bright expression of mesenchymal lineage markers and immunoregulatory properties. hAFSCs, seeded onto hydroxyapatite scaffolds and subcutaneously implanted in nude mice, played a pivotal role in mounting a response resulting in the recruitment of host's progenitor cells forming tissues of mesodermal origin such as fat, muscle, fibrous tissue and immature bone. Implanted hAFSCs migrated from the scaffold to the skin overlying implant site but not to other organs. Given their *in vivo*: (i) recruitment of host progenitor cells, (ii) homing towards injured sites and (iii) multipotentiality in tissue repair, hAFSCs are a very appealing reserve of stem cells potentially useful for clinical application in regenerative medicine.

© 2011 Elsevier Ltd. All rights reserved.

1. Introduction

Human mesenchymal stem cells (hMSCs) constitute a population of multipotent adherent cells able to give rise to multiple mesenchymal lineages such as osteoblasts, adipocytes, or chondrocytes [1]. So far, the most common source of hMSCs has been the bone marrow (BM), however BM-MSCs harvesting and processing exhibit major drawbacks and limitations, thus the identification and characterization of alternative sources of hMSCs are of great relevance. MSC can be found in adult tissues or in fetal tissues like umbilical cord blood, amniotic membrane and amniotic fluid (AF) [2,3]. Human amniotic fluid stem cells (hAFSCs) are a promising cell source that is abundantly available and contain pluripotent stem cells able to differentiate in different lineages [2,4]. The recent isolation of fetal stem cells from several sources either at early stage of development or during the later trimester of gestation, provides strong support to

the notion that fetal stem cells, including hAFSCs, may be biologically closer to embryonic stem cells. Human AFSCs may represent intermediates between embryonic stem cells and adult hMSCs, at least regarding proliferation rate and plasticity features [4]. These characteristics confer an advantage over postnatal MSCs derived from adult bone marrow [5]. Fetal stem cells are particularly appealing for clinical applications; these cells are readily isolated from tissues normally discarded at birth, avoiding ethical concerns that plague the isolation of embryonic stem cells [6]. These cells harbor a high proliferative capacity and the potential to differentiate into cells of all three embryonic germ layers [7]. The fact that hAFSCs are not teratogenic and do not raise the ethical concerns associated with human embryonic stem cells, make them an optimal tool to study and use in regenerative medicine and human genetic diseases.

Amniotic fluid has been used to screen fetal genetic and congenital diseases for many years [8]. The volume and composition of AF change during the pregnancy; contact between AF and compartments of the developing fetus explain the presence of different cell types [5]. The population of cells in AF is heterogeneous; the cells, mostly of epithelial nature, derive either from the developing fetus or from the inner surface of amniotic membrane [5]. It has been shown that these cells can be considered as

* Corresponding author. Department of Oncology, Biology, and Genetics, University of Genova, National Cancer Research Institute, Largo Rosana Benzi 10, 16132 Genova, Italy. Tel.: +39 010 5737241; fax: +39 010 5737257.

E-mail address: chiara.gentili@istge.it (C. Gentili).

¹ These two authors contributed equally to the work.

multipotent stem cells as they express several stem cell-specific markers such as Oct-4, Nanog and SSEA-4 but not SSEA1 and 3 [7,9]. Moreover, hAFSCs exhibit typical mesenchymal markers and they are negative for hematopoietic markers [2,4]. The presence of these markers despite to the pluripotent gene expression demonstrates that AF derived progenitor cells are not so primitive as embryonic stem cells, rather they maintain a potential of adult stem cells.

In the last years, different groups studied and used hAFSC for several tissue-engineering applications [10]. In the present study, we describe the *in vitro* isolation and characterization of hAFSC from second-trimester of AF samples and we report the stability in morphology, karyotype, clonogenicity, pluripotency and mesenchymal markers profile and immunomodulatory properties of the cells at early and late stage of cell culture. *In vivo* studies revealed that isolated hAFSCs, seeded into hydroxyapatite (HA) scaffolds and subcutaneously implanted in nude mice, left the scaffold by the first week. The explanted constructs were populated of murine cells able to generate different types of mesenchymal-derived tissues, as recently described with murine MSC [11,12].

2. Materials and methods

2.1. Cell culture and AFSC growth kinetics determination

Amniotic fluid was obtained by amniocentesis performed between 15 and 17 weeks of gestation for fetal karyotyping from the clinical cytogenetic laboratory (Ospedale Galliera, Genoa). All samples (20 different amniocentesis donors) were collected after obtaining written informed consent. Amniotic fluid cells were isolated by centrifugation of amniotic fluid; cell pellets were resuspended in the expansion medium α -MEM (Gibco-Invitrogen, MI, Italy), 20% of Chang Medium (Chang B + Chang C, Irvine Scientific, CA), 15% of fetal bovine serum (FBS) (Gibco-Invitrogen, MI, Italy), 1% of penicillin/streptomycin (Euroclone, MI, Italy) and L-glutamine (Euroclone, MI, Italy). After 5–6 days, non-adherent cells and debris were discarded and adherent cell cultivated until 70% confluence. Adherent cells were detached from the plastic plate using a trypsin-EDTA solution (Sigma, MI, Italy) for 5 min at 37 °C and re-plated; culture medium was changed 3 times a week. At each culture passage the cells were detached pooled, counted, and re-plated. The cumulative cell doublings of each cell populations were plotted against time in culture to determine the growth kinetics of hAFSCs.

To evaluate CFU frequency, 100 μ l of the original amniotic fluid suspension were plated in 100 mm plastic petri dishes. The first medium change was made after 5 days and then twice a week. After 2 weeks of culture, cells were washed with PBS pH 7.2, fixed with 3.7% formaldehyde in PBS, stained with 1% methylene blue in borate buffer (10 mM, pH 8.8) for 30 min, washed with distilled water, and the colonies counted. All determinations were performed in duplicate on three different primary cultures.

During the expansion of hAFSCs in standard conditions, the cell plating density was 4000 cells/cm² [13]. In some experiments, to test the influence of a different cell plating density on cell growth and maintenance of a clonogenic potential, cells were plated also at clonogenic density (10 cells/cm²) and passaged the culture every 2 weeks. CFU analysis and cell counting was performed every 2 weeks on three different primary cultures.

2.2. Gene expression analysis of hAFSCs

Total RNA was extracted from hAFSC using Trizol reagent according to the manufacturer's instructions (Invitrogen, CA, USA). Reverse transcription reactions were performed in a 20 μ l volume with 2 μ g of total RNA (Superscript first-strand synthesis system, Invitrogen, CA, USA). Semiquantitative RT-PCR was performed using the primers reported in Table 1.

2.3. Karyotype analysis of hAFSCs

The hAFSCs culture was performed at 25% confluence in SlideFlask (NUNC). The cells were then incubated in Ham's F10 (Celbio) with 0.1 mg/ml colcemid (Sigma) for 3h. The medium was removed and hypotonic solution (0.075M KCl, 0.017 M Na-citrate) added. Cells were fixed with ethanol:methanol:acetic acid (1:2:1) and dried at 25 °C and 45% humidity. Metaphase spreads were analyzed after staining with quinacrine (Sigma) for karyotyping. Analysis was performed on three different primary cultures counting 50 metaphases for each sample [14].

2.4. Monoclonal antibodies (mAbs) and reagents

The murine anti-human anti-CD45 mAbs (TA218/12, IgM), the anti-CD31 mAb (89D3, Ig2a), the anti-CD16 mAbs (NK1, IgG1), the anti-CD18 mAb (70H12, IgG2a), the anti-CD54 mAb (ICAM1, clone SM89, IgM), the anti-CD44 mAbs (T61/12, IgG1)

Table 1
RT-PCR primers.

Oct-4 245 bp (TA 55 °C)
F 5'-CGTGAAGCTGGAGAAGGAGAAGCTG-3'
R 5'-CAAGGGCCGACGCTCACACATGTTCC-3'
SCF 275 bp (TA 55 °C)
F 5'-CCATTGATGCCTTCAAGGAC-3'
R 5'-CTTCCAGTATAAGGCTCCAA-3'
Rex-1 298 bp (TA 64 °C)
F 5'-GCTGACCACCAGCACACTAGGC-3'
R 5'-TTTCTGGTGTCTTGTCTTTGCCCC-3'
Nanog 163bp (TA 61 °C)
F 5'-GCTGAGATGCCTCACACGGAG-3'
R 5'-TCTGTTTCTTGACTGGGACCTTGTC-3'
GAPDH 451bp (TA 59 °C)
F 5'-ACCACAGTCCATGCCATCAC-3'
R 5'-TCCACCACCTGTGTCTGTA-3'

were obtained in our laboratory as described [15]. The anti-CD3 mAb (UCHT-1, IgG1) was from Ancell (Bayport, MN55003, USA). The anti-HLA class-I W6/32 (IgG2a), the anti-SH2 (CD105, IgG1), the anti-SH3 (CD73, IgG2b), the anti-SH4 (IgG1), the anti-CD34 (clone IgG1) the anti-CD11a (LFA1 α , TS1.22, IgG1), the anti-CD18 (LFA1 β , TS1.18, IgG1) and the anti-CD40 producing hybridomas were purchased from the American Type Culture Collection (ATCC, Manassas, VA). Anti-HLA-ABC mAb (clone 3A3, IgM) and anti-CD14 mAb (63D3, IgG1) were kindly provided by E. Ciccone (Institute of Anatomy, University of Genoa) and D. Vercelli (Scientific Institute San Raffaele, Milan) respectively. The anti- β 1 integrin (CD29) mAb (3E1, IgG1) was a kind gift of Dr L. Zardi (IST-Genoa). The anti-ICAM2 and anti-ICAM3 mAbs were from Bender MedSystem (CA 94010, USA). The anti-prolyl-4-hydroxylase mAb (clone 5B5, IgG1) was purchased from Dako (Glostrup, Denmark). The anti-human CD146 (clone P1H12, IgG1), and the anti-CD56 (clone Leu19, IgG1) were from BD PharMingen, the anti-CD90 (clone Thy-1A1, IgG2a) was from R and D System Inc. (Minneapolis, USA), the anti-CD80 (clone P1.H5.A1.A1, IgG1), the anti-CD86 (clone BU63, IgG1) and the anti-HLA-DR (clone TDR 31.1, IgG1) mAbs were from Ancell Corp. (Bayport, MN, USA). The anti-murine (m) mAbs were APC conjugated-CD31 (clone 390 from Ebioscience, San Diego, CA, USA), FITC-conjugated-CD14 (clone rmC5-3, BD PharMingen), PE-conjugated-CD146 (clone P1H12, from Santa Cruz, Biotechnology, Heidelberg, Germany), mCD90 (clones 30-H12), mCD106 (clone 429), mCD45 (clone 104) (PE-conjugated) were from BD PharMingen (San Diego, CA, USA). Phytohemagglutinin (PHA) and Staphylococcal enterotoxin B (SEB) were from Sigma Chemicals Co. (St. Louis, MO, USA) and used at 1 μ g/ml as the optimal concentration to induce proliferation of T cells. Complete medium for culture of peripheral blood mononuclear cells (PBMC) was composed of RPMI1640 (Biochrom, Berlin, Germany) with 10% of fetal calf serum (FCS, Biochrom, Berlin, Germany) supplemented with 1% antibiotics (penicillin and streptomycin) and 1% L-glutamine (Biochrom, Berlin, Germany).

2.5. Immunofluorescence and cytofluorimetric analysis

Immunofluorescence on cultured hAFSCs either at an early stage (20 db, 25 days) or at a late stage (60 db, 120 days) or on PBMC was performed with the above described mAbs followed by the addition of anti-isotype specific goat anti-mouse (GAM) antisera (Southern Biotechnology, CA, USA) conjugated with phycoerythrin (PE), or fluorescein isothiocyanate (FITC) or AlexaFluor647 (Invitrogen) as indicated. Control samples were stained with isotype-matched irrelevant mAb (Becton Dickinson) followed by anti-isotype specific GAM-PE or GAM-FITC or GAM-Alexa-Fluor647. Samples were run on Cyan ADP cytofluorimeter (Beckman-Coulter, Brea CA, USA). Data were analyzed using the Summit 4.3.1 computer program and are expressed as Log fluorescence intensity vs. number of cells or as mean fluorescence intensity (MFI) expressed in arbitrary units (a.u.) [16].

2.6. hAFSCs-PBMCs co-culture experiments

PBMC were separated from blood samples of healthy donors as described [16]. hAFSCs were co-cultured with 10⁵ PBMC at different AFSC:PBMC ratios (1:2, 1:4, 1:8, 1:16 and 1:32) in medium alone or in the presence of anti-CD3mAb (JT3A, IgG2a), PHA (1 μ g/ml) or SEB (1 μ g/ml) in U-bottomed microplates in 200 μ l and proliferation was evaluated at 3, 5 and 7 days of culture. Cell proliferation was assessed after labeling PBMC with carboxy fluorescein succinimidyl ester (CFSE, Invitrogen s.r.l. Molecular Probes, Carlsbad, CA) according to manufacturer's instructions. Proliferation was assessed by cytofluorimetric evaluation of progressive loss of CFSE with increasing culture passages proportional to cell division, on gated T cells labeled with anti-CD3 mAb (UCHT-1, IgG1) [16,17]. In preliminary experiments, this assay gave comparable results to assays based on uptake of radiolabelled thymidine. In some experiments, 10 ng/ml of recombinant IL2 (Invitrogen) was added on day 5 to determine at day 7 the responsiveness of lymphocytes to this cytokine. To determine the role of hAFSC-PBMC contact in regulating T cell proliferation, in some

experiments, PBMC were seeded on Millicell transwell (TW) with 0.3 μm pores (Millipore Corporation, Billerica, MA) put in 24w plates with hAFSCs seeded on the bottom to avoid hAFSC-PBMC contact.

2.7. In vivo analysis of cell recruitment

Cell recruitment in in vivo implants was assayed according to a protocol previously optimized in our laboratory [18]. Briefly, 2.5×10^6 hAFSCs were loaded on a 100% hydroxyapatite (HA) $4 \times 4 \times 4$ mm support (EngiPore-EP, FinCeramica, Faenza, Italy) and the constructs were implanted subcutaneously on the back of twelve nude CD-1 nu/nu mice (Charles River- Calco, LC, Italy). Animals were sacrificed 1, 2, 4 and 8 weeks after implantation, and the grafts removed and processed for histological analysis to investigate and analyze tissue formation. The scaffolds were harvested, washed in HBSS/30 mM HEPES (Euroclone, MI, Italy) plus penicillin and streptomycin and digested twice with 100 U/ml type I and II collagenase (Biochrom, AG Berlin, Germany) plus 2.5% Trypsin (Gibco, MI, Italy) for 40 min at 37 °C [19]. At least 8×10^5 cells obtained from the digestions were analyzed by cytometer using mAb against mouse mCD90, mCD106, mCD45, mCD31, mCD14 and mCD146 in addition to the mAb against the human antigens above reported. For each time point we implanted three mice with four scaffolds, two scaffolds were loaded with hAFSCs and two control scaffolds were empty.

The care and the use of the animals were in compliance with the laws of the Italian Ministry of Health and the guidelines of the European Community.

2.8. In vivo cell tracing of hAFSCs

Cells were trypsinized, suspended ($10^6/\text{ml}$) in serum free medium and incubated with 10 μM CM-Dil (Invitrogen, Molecular Probes, MI, Italy), for 10min at 37 °C plus 15min at 4 °C. After three washes in PBS, 2.5×10^6 labeled cells were loaded into each scaffold. Constructs were subcutaneously implanted in nude mice for 1 week. Explanted constructs were digested as reported above, cells were harvested and analyzed at flow cytometer for CM-Dil fluorescence and for the presence of HLA-ABC mAb, followed by GAM- AlexaFluor647.

Cell suspensions were prepared from the skin overlying the implant (1 cm \times 0.5 cm flap) [20] and from kidney [21], liver [22] and spleen [23], using enzymatic digestion. CM-Dil fluorescence intensity of recovered cells was analyzed at Cyan ADP (Beckman-Coulter, Hyalea, USA). Cells isolated from organs of not implanted nude mice were used as negative control. The presence of hAFSCs in derma was also demonstrated by CM-Dil fluorescence observed on histological sections.

2.9. Histological analysis

Formalin-fixed HA scaffolds were processed as reported [11]. Briefly, samples were decalcified with Osteodec (Bio-Optica, Milano, Italy) and embedded in paraffin using standard histological procedure. Four-micrometer serial sections were cut; sections were stained with hematoxylin and eosin (H&E) to reveal tissue formation. The histology sections were analyzed using a brightfield light microscope (Axiovert 10, Zeiss, Germany) equipped with a digital camera (Olympus DP10, Olympus Optical, Japan). Images were acquired at 100 \times , 200 \times and 400 \times magnifications.

2.10. Statistical analysis

The data were analyzed by two-tailed *t*-tests. A *p*-value ≤ 0.05 was considered to be statistically significant.

3. Results

3.1. Isolation and expansion of hAFSCs

The morphology of the total adherent population of cells isolated from 20 samples of human amniotic fluid was monitored during the culture. In the initial culture dishes (passage 0 of the primary culture) this population displayed a heterogeneous

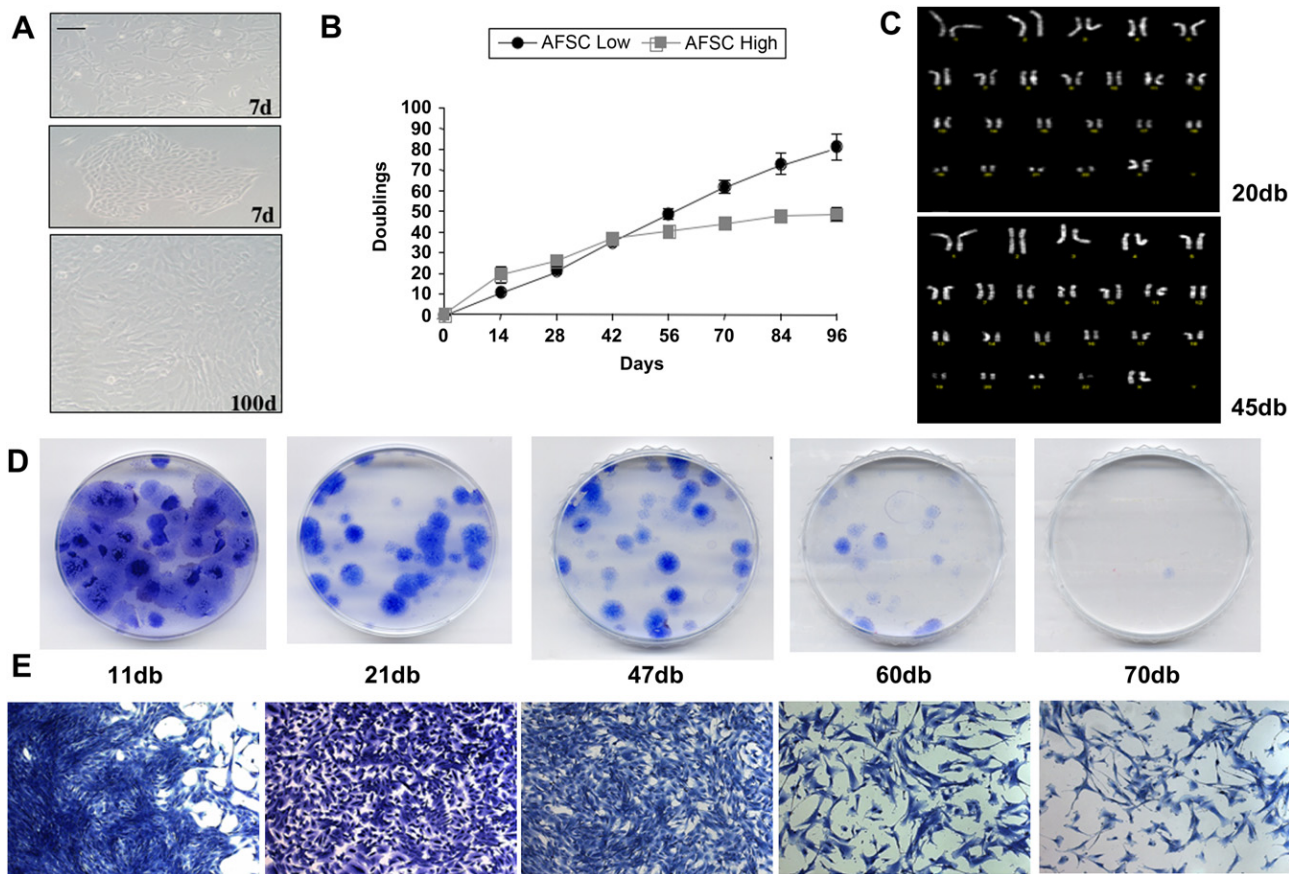


Fig. 1. Phenotypic characterization of hAFSCs in culture: (A) Cell morphology: fibroblast-like cells (upper panel), epithelial-like cells (middle panel) at 7 days of culture; homogeneous spindle cells at 100 days of culture (lower panel). (B) The growth curves of low density ($10\text{cells}/\text{cm}^2$) plated hAFSCs (black line) compared to high density ($4000\text{ cells}/\text{cm}^2$) plated hAFSCs (grey line). (C) Karyotype analysis at 20 db and at 45 db. (D) hAFSCs clonogenic potential: (CFU assay) and (E) cellular morphology of the colonies obtained. All the results are representative of three independent experiments.

morphology and two main types of cells were observed; epithelial-like and fibroblastic-like. After one passage all hAFSCs in the culture dishes presented a fibroblast-like morphology (Fig. 1A).

We obtained a median of 3 CFU/ml of amniotic fluid, confirming the low number of mesenchymal progenitors present in the amniotic fluid that can be effectively expanded in culture. Nevertheless, these few MSC cells were sufficient to obtain extremely high numbers of “in vitro expanded” hAFSCs. After the first passage, cells were re-plated both under clonogenic conditions (10 cells/cm²) and split every 2 weeks, and at high density (4000 cells/cm²). In both culture conditions, we never allowed the cells to reach confluence. During the first 40 days of culture the cell doubling time was between 24 and 36 h in all culture conditions with a tendency to a higher proliferation rate not statistically significant observed in the high density passaged cultures during the first two weeks. During the third month of culture, in the same high density cultures the cell doubling time dramatically decreased while in the cultures passaged at clonal density remained essentially unchanged (Fig. 1B). Despite to the high proliferative capacity of hAFSCs, we did not observe any karyotypic abnormality; indeed, hAFSCs analyzed at 0, 20 db (25 day culture) and 45 db (86 day culture), displayed a normal karyotype (Fig. 1C). In the clonal density passaged cultures, hAFSCs gradually lost their ability to generate new colonies and the size of the colonies progressively decreased with the increase of the cell doublings (Fig. 1D). Only after 60 db we start to observe some flattened senescent cells (Fig. 1E) [24].

3.2. Phenotype of hAFSCs

Human AFSCs were further analyzed for the expression of a series of stem cell-specific or “stemness” marker. RT-PCR analysis showed that hAFSC cells at 20 db and 45 db consistently expressed

Oct-4, Nanog, Rex-1 and SCF genes (Fig. 2A). Characterization by flow cytometry of early 20 db (25 days) and late population 60 db (120 days) of hAFSCs confirmed the expression of “genes”, such as SSEA-4, SOX2 and Oct3/4 (Fig. 2B). Moreover, the cells showed bright expression of CD146, CD56, CD73, CD105, CD44, CD90, CD29 and HLA-ABC. These markers were expressed at 20 db in culture and were maintained, except CD73 that was enhanced at late stage, while the neuroectodermal crest marker CD56 was lost along culture. Moreover, hAFSCs did not express the hematopoietic lineage-specific markers CD45, nor co-stimulatory molecules like CD80 and CD86 and HLA-DR (Fig. 2C) or molecules involved in cell-to cell interactions as ICAM2 and ICAM3 (not shown). However, they expressed at low levels molecules relevant for interaction with leukocytes as CD54 (ICAM1) (25–45%, n = 5) and CD40 (70–85%, n = 5) antigens [17]. It is of note that the percentage of cells expressing these antigens was strongly reduced in culture. Indeed, after 60 db only a small fraction of hAFSCs expressed CD40 (10–20% on 60 db vs, 50–85% after 20 db, n = 5) or CD54 (20–25% on 60 db vs 25–45% after 20 db n = 5).

3.3. hAFSCs inhibit T-cell proliferation

We analyzed whether hAFSCs can inhibit T cell proliferation as reported for MSC isolated from bone marrow. To this aim, peripheral blood lymphocytes were stimulated with PHA or anti-CD3mAb (polyclonal stimuli for T cells) or SEB (oligoclonal stimulus for T cells) and co-cultured with hAFSC in the presence of grading amount of hAFSCs. A representative experiment out of 8 performed is shown in Fig. 3A. Interestingly, we found that hAFSCs strongly reduced T cell proliferation triggered through the polyclonal stimulus PHA (Fig. 3A). Indeed, about 80% of T cells (range 60–85%, n = 8) were proliferating on day 4 of culture upon stimulation with

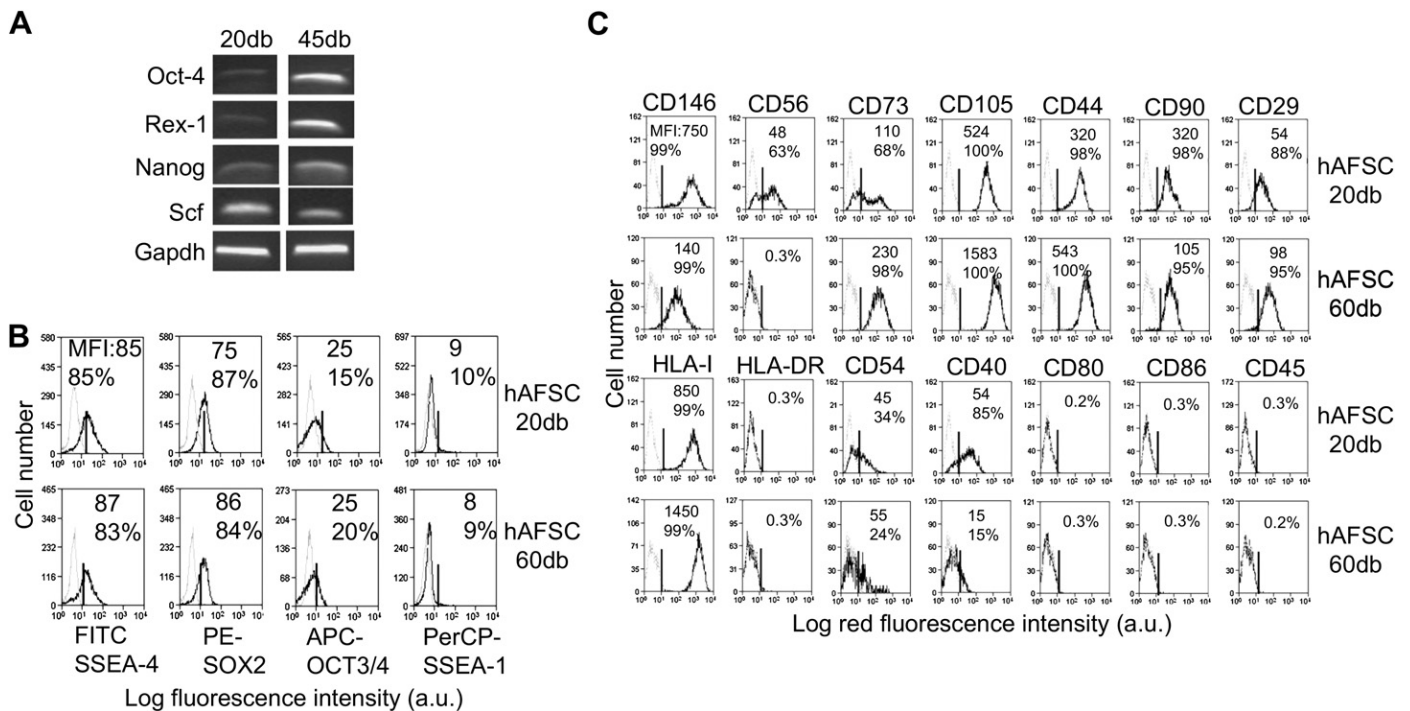


Fig. 2. Cytofluorimetric analysis of phenotype of hAFSCs. (A) RT-PCR expression of Oct-4, Res1, Nanog, and Scf at 20 and at 45 db. (B) Intra-cytoplasmic expression of the indicated transcription factors in hAFSCs after 20 db (upper subpanels) or 60 db (lower subpanels). In each subpanel, cells stained with an unrelated mAb matched for isotype (grey histogram) or with mAbs to the indicated molecules (black histograms), the mean fluorescence intensity (MFI) and the percentage of positive cells are shown as well. (C) Surface expression of the indicated molecules. Human AFSCs were stained with mAbs to different markers (black histograms). In each subpanel, it is shown (grey histogram) the isotype matched mAb used as control. The percentage of positive cells beyond unstained cells (black bar) and MFI are indicated. Results are expressed as Log fluorescence intensity arbitrary units (a.u.) vs number of cells and are representative of five independent experiments.

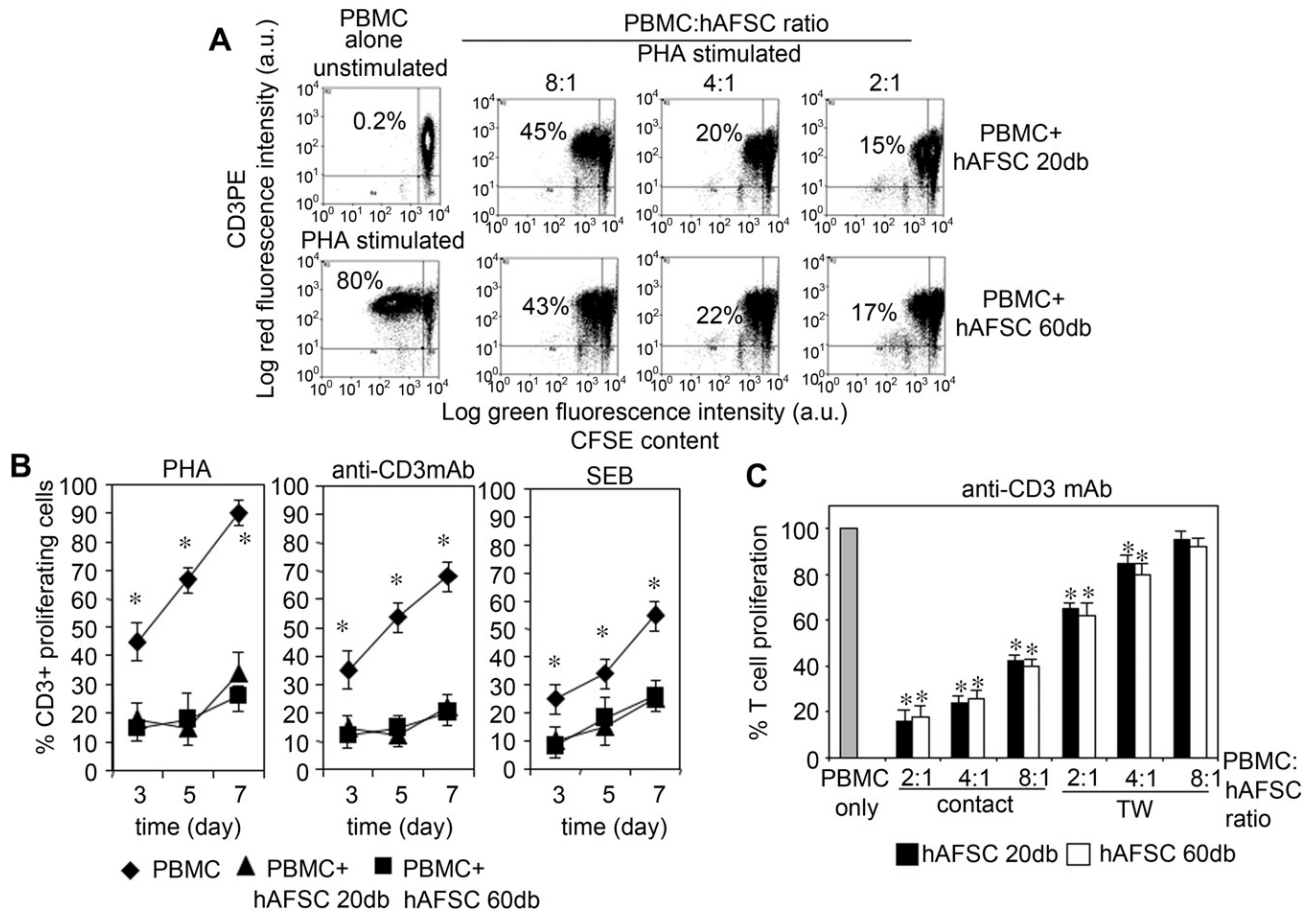


Fig. 3. Human AFSCs inhibit T cell proliferation. (A) Peripheral blood mononuclear cells (PBMC) labeled with CFSE were cultured on hAFSC at 20 doubling time (db) (upper quadrants) or at 60 db (lower quadrants) at different PBMC:hAFSCs ratios (8:1, 4:1 and 2:1) and stimulated with PHA (1 μ g/ml). Proliferation was assessed as decrement of CFSE cell staining in CD3⁺ T cells. Each quadrant was subdivided in four regions (lower left: CD3 negative proliferating cells; lower right: CD3 negative non proliferating cells; upper left: proliferating CD3⁺ cells; upper right: non proliferating CD3⁺ cells). The first upper quadrant on the left indicates basal proliferation of PBMC without PHA in the absence of hAFSCs while the lower first quadrant the proliferation of PBMC alone in the presence of PHA. In each quadrant the percentage of proliferating T cells is shown. Data are expressed as Log green fluorescence intensity vs Log red fluorescence intensity arbitrary units (a.u.) and are representative of 8 independent experiments with similar results. (B) Kinetics of proliferation of CD3⁺ T cells stimulated with PHA (left) or anti-CD3 mAb (middle) or SEB (right), alone (rombs) or with hAFSCs at 20 db (triangles) or with hAFSCs at 60 db (squares) at the PBMC:hAFSCs ratio of 2:1. On day 5, 10 ng/ml of IL2 was added and proliferation of T cells analyzed on day 7. T cell proliferation was assessed as in (A). Results are shown as the mean \pm SD of 8 independent experiments. (C) PBMC alone (grey bar) was stimulated with anti-CD3 mAb or with hAFSCs in contact or separated by a transwell (TW) at different PBMC:hAFSCs ratios as indicated and proliferation was evaluated on day 3. hAFSCs at 20 db (black bars) or at 60 db (white bars) were used for comparison. Data are expressed as % of T cell proliferation normalized to proliferation of PBMC in the absence of hAFSCs. Proliferation was assessed as in panel A. * p < 0.05 by student t test analysis on 8 independent experiments.

PHA whereas in co-culture with hAFSCs at 20 db a strong inhibition of T cell proliferation was detected (from 80% to 15% of proliferating T cells). It is note that the inhibition of T cell proliferation was dose dependent reaching a maximum when PBMC were co-cultured with hAFSCs at 2:1 ratio (about 15% of proliferating T cells on day 4, range 10–35%, n = 8). At PBMC:hAFSCs ratio of 8:1 T cell proliferation was 45% (range 40–60%, n = 8) of that observed in absence of hAFSCs (Fig. 3A) and responsiveness of T cells to PHA was completely restored at 32:1 PBMC:AFSCs ratio (not shown). Furthermore, it appeared that hAFSCs maintained this immunosuppressive effect throughout all their in vitro expansion up to at least 60 db (Fig. 3A, compare upper with lower dot plots). On day 5, also T cell proliferation to anti-CD3mAb or SEB was strongly reduced by the co-culture with hAFSCs (T cell proliferation of 55% vs 15% to anti-CD3mAb or 35% vs 17% to SEB) (Fig. 3B). The addition of exogenous IL2 on day 5 further increased T cell proliferation, assessed on day 7, either when PBMC was cultured alone or with hAFSCs (Fig. 3B). However, T cells in the presence of hAFSCs proliferated at a very lower extent compared to T cells cultured without hAFSCs (Fig. 3B, compare results reported on day 7). In

parallel experiments, we analyzed whether hAFSCs could exert any inhibition on T cell proliferation when PBMC were separated from hAFSCs by a transwell (TW) (Fig. 3C). In this culture system, hAFSCs were less effective in inhibiting T cell proliferation (that decreased from 100 to 65% for CD3-mediated stimulation at PBMC:hAFSC ratio of 2:1, range 50–75%, n = 8) compared to PBMC-hAFSCs cultured in contact (from 100 to 15% at PBMC-hAFSCs ratio of 2:1, range 10–25% n = 8) (Fig. 3C). Again, it appeared that hAFSCs maintained this level of immunosuppressive effect throughout all their in vitro expansion up to at least 60 db (Fig. 3C).

3.4. In vivo tracing of hAFSCs

We labeled hAFSCs with CM-Dil to follow their fate in vivo. Indeed, CM-Dil labeled hAFSCs (Fig. 4A) were seeded into scaffolds and the constructs implanted in nude mice. After 1 week mice were sacrificed, and cell suspensions were obtained by enzymatic digestion from the scaffold and from different organs including skin, spleen, liver and kidney. Recovered cells were run on a cyto-fluorimeter to detect red fluorescence of CM-Dil⁺-hAFSCs. Cell

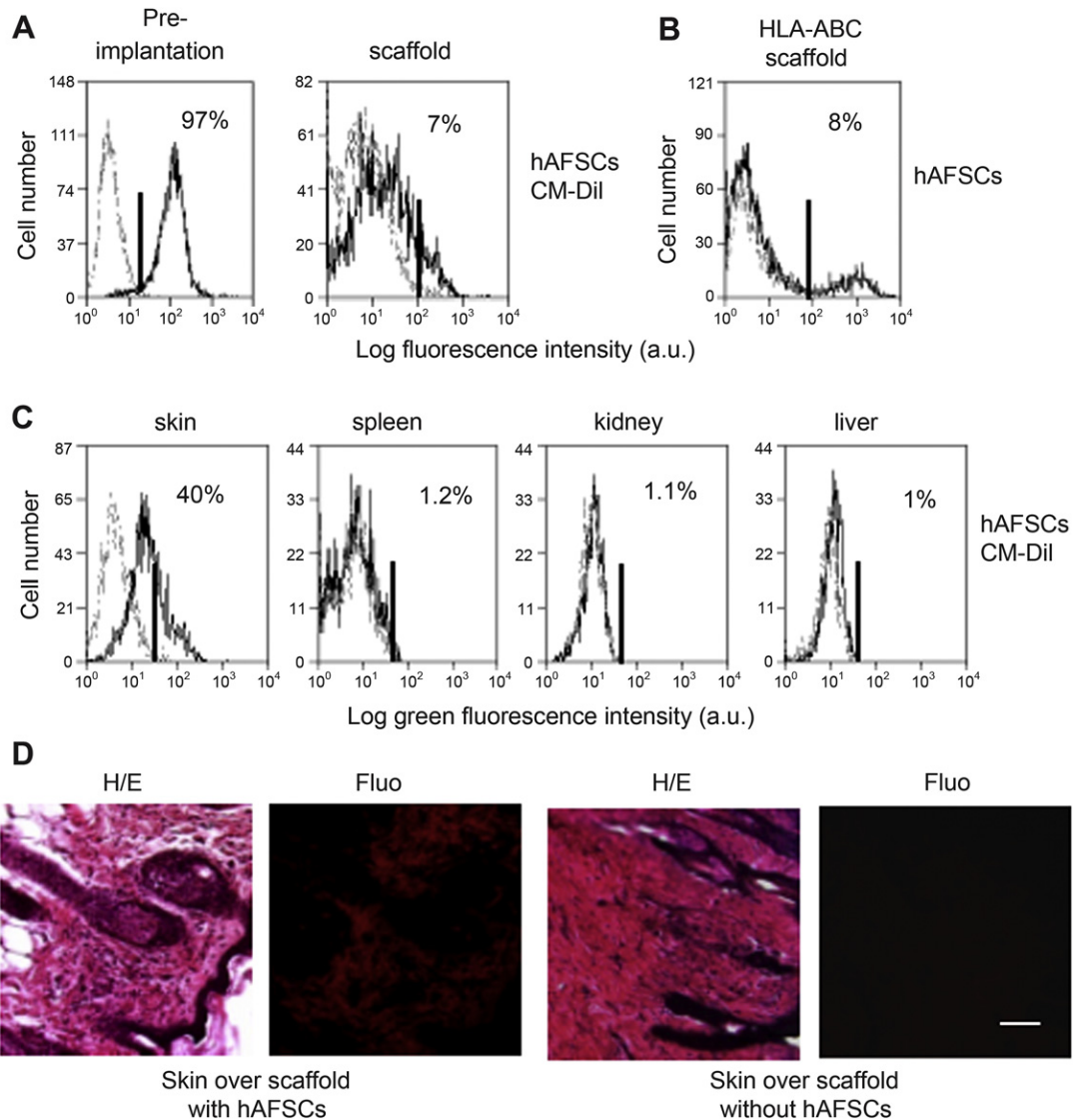


Fig. 4. “in vivo” tracing of hAFSCs: (A) (left panel) CM-Dil labelled hAFSCs before implantation: black histogram is meant for the red fluorescence of labeled hAFSCs respect to unlabeled cells (grey histogram). (A) (right panel) presence of CM-Dil+ hAFSCs in cells extracted from the scaffold: black histogram shows cells extracted from hAFSCs loaded biomaterials, grey histogram is for cells extracted from empty biomaterials. (B) The presence of residual hAFSCs is investigated by the retrieval of HLA-ABC antigen in extracted cells at 1 week; black histogram shows HLA-ABC positive cells, grey histogram is the isotype control. (C) hAFSCs (CM-Dil positive cells) in the skin adjacent to the implant site, in spleen, kidney and liver. The percentage of positive cells beyond unstained cells (black bar) is indicated; black histograms show the digested organs of implanted mice, grey histograms show organs of not implanted mice. (D) H&E histology staining and red fluorescence of CM-Dil+ hAFSCs retrieved in derma. Bar: 200 μ m. Analyses of four independent experiments.

suspensions isolated from skin, kidney, liver and spleen of not implanted nude mice were used as negative control. We found that at 1 week from implantation 5–10% of hAFSCs were retrieved in the scaffold (Fig. 4A–B), whereas high percentages of CM-Dil+ cells (about 40%) were recovered from the skin overlying the implant site (Fig. 4C). We did not find hAFSCs in the spleen, kidney and liver (Fig. 4C). Analysis of the recovered skin showed that hAFSC (CM-Dil positive cells) were present in the derma over scaffold loaded with the hAFSC, while no fluorescence signal was detected in the derma over empty scaffold (Fig. 4D).

3.5. Characterization of cells and tissue formation within AFSC-constructs

To determine the fate of the implanted hAFSCs and the type, nature and origin of the tissues neo-formed within the scaffold pores, we implanted hAFSC-constructs in nude mice and we

determined by cytofluorimeter the human or murine origin of cells present into scaffold at different time intervals. Further, the tissue formed within the scaffold pores was analyzed by histology.

Constructs were harvested at 1, 2 and 4 weeks after implantation, and enzymatic digested to obtain single cell suspensions. After 1 week, only 5–10% of the recovered cells expressed HLA-ABC (Fig. 4B). At 2 weeks from implantation, all cells recovered were HLA-ABC negative and they did not react with antibodies to human mesenchymal markers including CD73, CD90, CD105 and CD146 (Fig. 5A). On the other hand, these cells were positive for some murine antigens as CD90, CD106 (Fig. 5B). Analysis of cells harvested after 4 weeks from implantation, confirmed the absence of human cells, and importantly, recovered cells were positive for mCD90 and mCD106 surface markers (Fig. 5C).

Recovered cell suspension harvested from scaffold, were further cultured in vitro. We obtained in 4–7 days a quite homogeneous cell population of cells strongly expressing mCD90

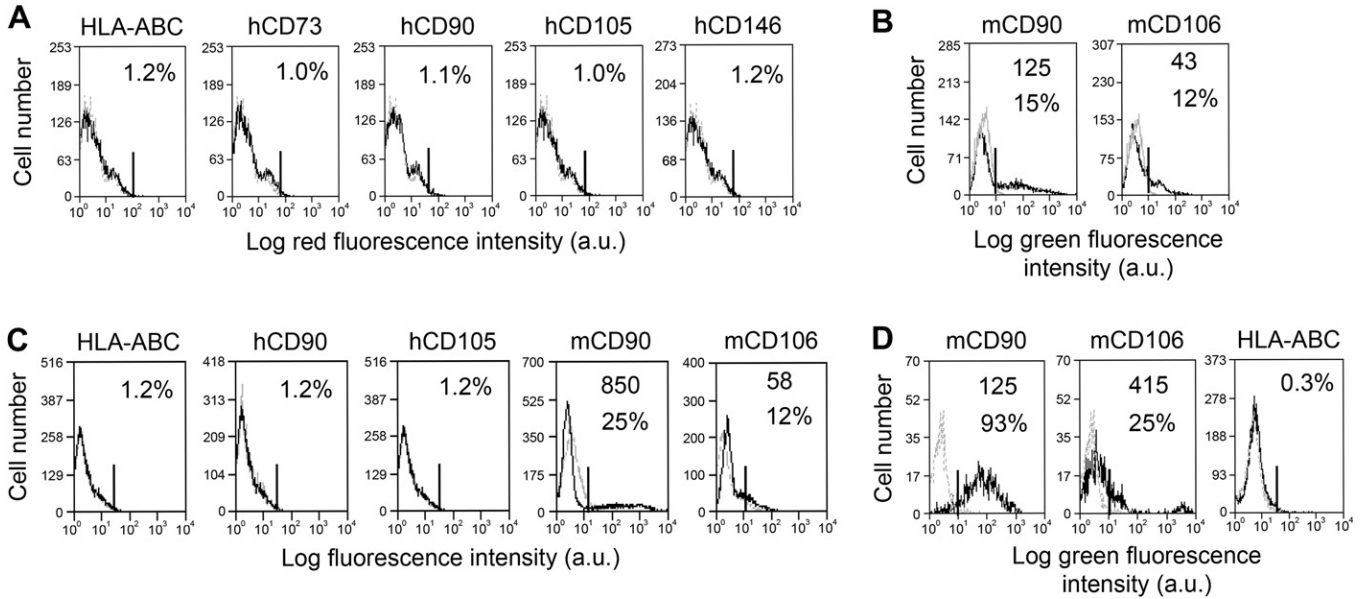


Fig. 5. Phenotype of cells harvested from implanted scaffolds. Ex-vivo constructs were collected at 2 weeks (A and B) and 4 weeks (C) and digested; cells were harvested and analyzed at cytofluorimeter for some human and mouse mesenchymal markers. Cells were stained with mAbs to the indicated human (h) or murine (m) antigens (black line); in each histogram, it is shown the isotype matched negative control (grey line). (D) Cells recovered from the 4 weeks scaffold were in vitro cultured for additional 7 days and analyzed for the expression of the indicated surface markers. The percentage of positive cells (gated by black bar in each histogram) and the MFI of these cells are shown. Results are expressed as Log fluorescence intensity in arbitrary units (a.u.) vs number of cells and are representative of three independent experiments.

(Fig. 5D). It is of note that mCD106⁺ cells were still present in this culture.

When we compared the recruitment of host cells in empty and hAFSC-seeded scaffolds at different implantation times, we

observed that the expression of murine CD14 and CD31 decreased in both types of constructs, but in the scaffolds seeded with hAFSCs there was a significantly higher recruitment of CD14⁺ (Fig. 6A) and CD31⁺ (Fig. 6B) cells of host murine origin. On the other hand the

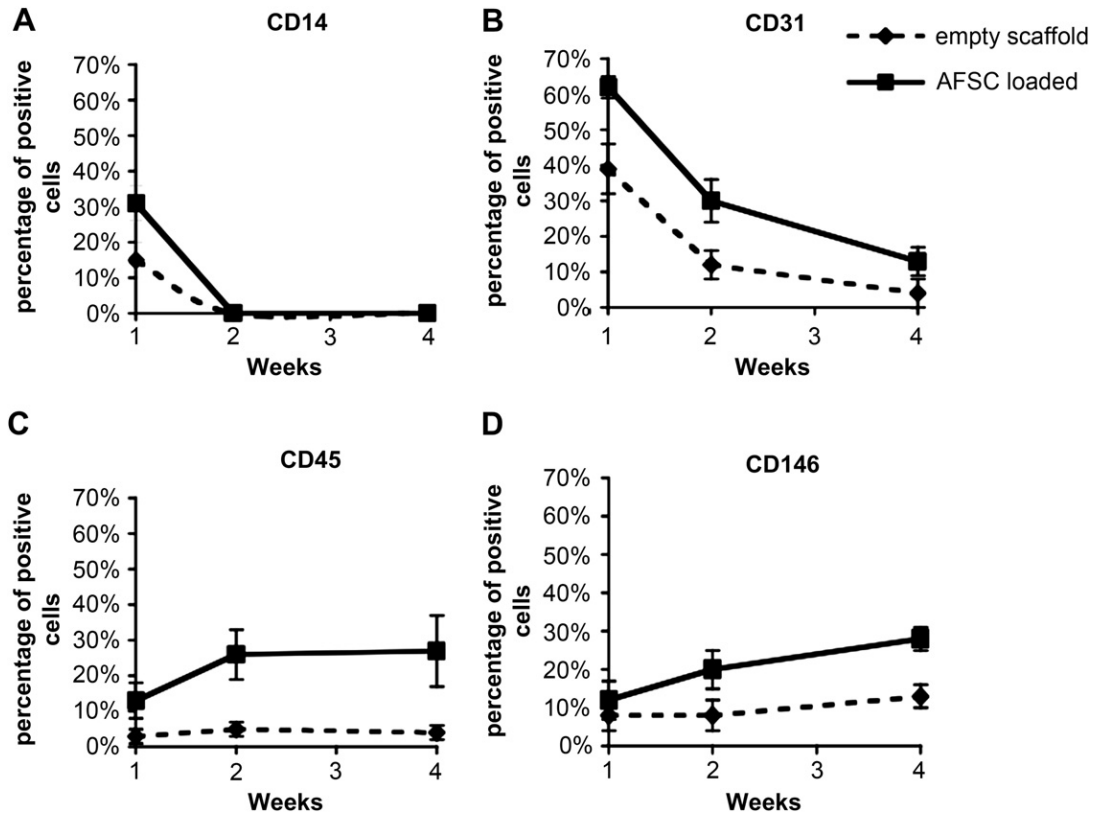


Fig. 6. Recruitment comparison between empty and hAFSC-seeded scaffolds through time. Cells harvested from 1, 2 and 4 weeks explanted scaffolds, were analyzed by cytofluorimeter for murine CD14 (A), CD31 (B), CD45 (C) and CD146 (D) antigens. Results are expressed as percentage of positive cells and are representative of three independent experiments.

percentage of CD45⁺ cells retrieved in hAFSC-seeded scaffolds increased with time, remaining low in the empty scaffolds (Fig. 6C). The number of CD146⁺ cells, present in hAFSC-seeded scaffolds, reached the 30% at 4 weeks, while remained stable at 8–12% in the empty scaffolds (Fig. 6D).

Finally, we analyzed at the different times the nature of tissues present within the pores of the hAFSCs seeded scaffolds after implantation *in vivo*. An initial (at 1 week) inflammatory reaction was clearly detectable in these scaffold constructs (Fig. 7A). Subsequently the formation of vessels and tissues was observed (Fig. 7C). While, the empty implanted control scaffold was poorly populated by cells and no organized tissues were evident (Fig. 7B). After 8 weeks, in the same scaffolds we observed a variety of different tissues of mesodermal origin: stroma (Fig. 7D), adipose tissue (Fig. 7E), muscle (Fig. 7F–G) and a tissue similar to immature bone (Fig. 7H).

4. Discussion

Recent findings point to amniotic fluid as a possible new source of multipotent stem cells [4]. Multipotent stem cells can be found in adult tissues or in fetal tissues such as the umbilical cord blood, amniotic membrane, or amniotic fluid [5]. Human AFSCs have intermediate properties between embryonic and adult MSC, which make them particularly attractive for regenerative medicine compared to other multipotent stem cell counterpart and gives them apparent advantages for accessibility, renewal capacity and multipotentiality and no ethical issues.

In this study, we have described the isolation and the extensive expansion of fetal mesenchymal stem cells from amniotic fluid. Human AFSCs maintained, at least up to 45 db, morphology, karyotype, stem cell gene transcription and MSC marker expression. In spite of the several works reporting an aneuploid karyotype in human and mouse MSC cultures after several *in vitro* passages [25,26], we observed a stability of the chromosomal asset even at late culture stages. Moreover, at late culture stages, the stem cell genes were still expressed as shown by RT-PCR and flow cytometry analysis.

As previously reported for hMSC, cell density is critical during *in vitro* expansion of hAFSCs. Passaging of the cells at low cell density strongly increased hAFSCs expandability through the maintenance

of their original morphology, given another proof of the staminal potential of these cells [24,27]. By re-plating the cells at low density, few milliliters of amniotic fluid can readily produce more than 100 million of cells to be potentially used for different clinical applications. Only after 60 db, we observed a drastic decrease of colony formation and some flattened senescent cells.

The cytofluorimetric analysis of the cultured cells showed that hematopoietic markers were not expressed. Mesenchymal markers were detected at early stage and maintained throughout the culture, with the exception of CD73, ecto-5-nucleotidase, whose expression was enhanced after 60 doublings. It has been described that the coordinate regulation of CD73 and its receptor may modulate the proliferation and CFU formation of murine MSC cells [28]. Moreover, it has been demonstrated that the adenosine generated by the CD73 activity plays an important tissue-protective role by attenuating inflammatory and apoptotic processes [28,29]. Thus, we could speculate that at late passage hAFSCs up regulate the CD73 in order to increase the production of adenosine. On the contrary, CD56 was lost at late passage hAFSCs cultures. As Mariotti et al. observed, CD56 was consistently expressed on a cell subset of human placenta MSCs and not in bone marrow MSCs [30,31]. The expression of CD56 by neuroepithelial and skeletal muscle cell lineage and the presence of this marker at early stage of hAFSCs culture could suggest a possible application of this source of cells in neuro and muscular differentiation protocols [32].

We also investigated the immunological properties of hAFSCs. These cells displayed immunosuppressive effects on T cell proliferation initiated through the engagement of CD3-T cell receptor complex or triggered by mitogen as PHA or bacterial toxins. This suggests that hAFSCs may down regulate both antigen dependent and independent stimulation of lymphocytes [33,34]. The lack of expression of HLA-DR and co-stimulatory molecules as CD80 and CD86 would suggest that hAFSCs are not able to stimulate allo-reaction and thus they could be good candidates for transplantation protocols. On the other hand, hAFSCs expressed detectable amounts of CD40 antigen. CD40 may interact with CD40 ligand expressed by lymphocytes leading to their activation as it happens during interaction between CD40⁺ dendritic cells and CD40 ligand⁺ T cells [35,36]. It should be noted that the expression of CD40 on hAFSCs was strongly reduced after 60 db, suggesting that long-term culture of hAFSCs would be more suitable

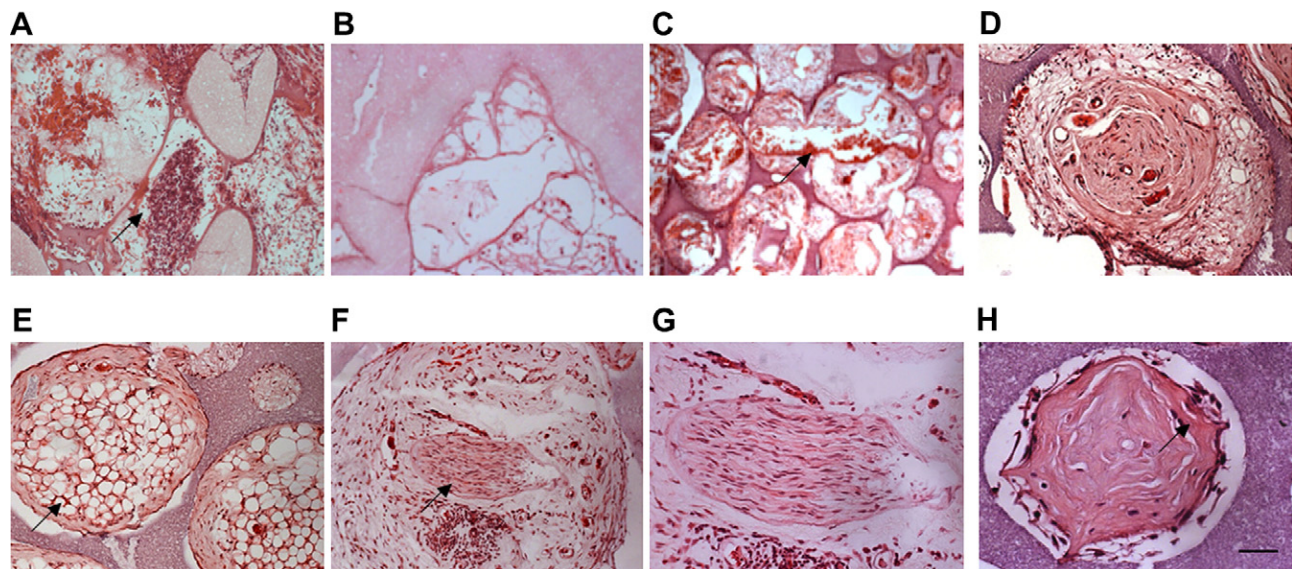


Fig. 7. Histology of explanted constructs. H&E analysis of hAFSC-constructs at 1 week (A), 4 weeks (C) and 8 weeks (D–H). Empty construct is the control (B). At 8 weeks, different types of mesenchymal tissues are shown: dense fibrous tissue (D), fat (E), muscle (F–G), and immature bone like tissue (H). Bar 200 μ m: C, Bar 100 μ m: A, B, D, E, F, Bar 50 μ m: G, H.

for transplantation lacking allo-stimulating molecules [37]. In addition, down-regulation of T cell proliferation was detected also when lymphocytes were not in direct contact with hAFSCs in a transwell culture system. This suggests that soluble factors may involve in hAFSCs-mediated inhibition of T cell proliferation. However, the inhibiting effect detected in a transwell culture system was significantly lower than that detected when hAFSCs-T cell interaction was allowed indicating that cell-to cell contact was needed to optimal immunosuppressive effect. It is of note that the direct and indirect inhibiting effect exerted by hAFSCs was still evident using the cells after 60 db, further reinforcing the idea that also long termed hAFSCs are suitable candidate to employ in regenerative medicine in allogeneic setting.

Some literature reports, including publications from our laboratory, indicated that signal from implanted stem cells can induce the mobilization into the site of a lesion of host stem/progenitor cells that can mediate the tissue repair [11,38,39]. We investigated the possible recruitment of host stem/progenitor by hAFSCs, we determined the *in vivo* fate of the implanted hAFSCs, the origin and the nature of the recruited cells and the cascade of events leading to the formation of new tissues. After 1 week, only few human cells were isolated from the implants, while at 2 weeks the whole cell population recovered from the scaffold was of murine origin and we could not retrieve any human cells.

The isolated murine cells were positive for CD90. CD90 is expressed on a variety of fibroblasts from different tissues, as a regulator of cell–cell and cell–matrix interaction and of cell motility. CD90 expression is important to mediate tissue repair, since prevent the wound to become a fibrotic lesion [40]. We would speculate that the CD90⁺ cells are host's cells that together with cytokines released by inflammatory cells such as CD45⁺ cells, also present in the lesion microenvironment, play a role in determining a milieu favoring the tissue reparative processes.

Cells extracted from late implants (2 and 4 weeks) were CD14⁻ and CD45⁺. Since CD45 is expressed on the surface of all leucocytes, while CD14 is found on cells of the myelo-monocytic line, one could speculate that at least part of the implanted hAFSC were phagocytosed by murine CD14⁺ cells during the first week, and that the resulting inflammatory cascade could had a role in attracting lymphocytes. The direct release of chemotactic molecules by the implanted hAFSC must also be considered as a possible alternative or complementary mechanism to explain the lymphocyte recruitment. Further, the absence of CD45⁺ cells in empty scaffolds indicates that the surgical procedure and the biomaterial alone are not sufficient to drive host cell mobilization and the regenerative cascade.

The retrieval of CD31⁺, CD146⁺ and CD106⁺ cells in late implants suggests that activated endothelium occurs when hAFSC are seeded onto scaffolds; moreover the expression of CD106 is the ulterior proof that microvascular endothelial cells are activated and ready to orchestrate localization and diapedesis of leukocytes during early stages of tissue inflammation [41]. In short, hAFSCs create a microenvironment where inflammation, vessel perfusion and recruitment of progenitor cells (circulating progenitors or niche progenitors coming from the adjacent sites of implantation) regenerate amorphous tissues.

Human AFSCs were detected in the skin overlying implant site but not in other organs, like spleen, kidney and liver. This would suggest that subcutaneously implanted hAFSCs migrated to the surgically wounded skin adjacent to the implantation site, but could not target distal organs by the systemic circulation, or that, at least, our *in vivo* tracing system was not so sensitive to detect the presence of very few cells that could have homed in those tissues. Recent papers reported that hAFSCs topically injected into different injured organs have a protective effect and are able to resolve the damage [42,43]. Moreover, many evidences show that hAFSCs

release paracrine factors able to accelerate the wound healing process by stimulating proliferation and migration of progenitors cells through the secretion of various cytokines and chemokines including IL-6, IL-8, TGF- β , VEGF and EGF [44]. Also data of our group show an active secretion of growth factors, chemokines involved in progenitor cells recruitment (paper in preparation).

The histology of the recovered implants confirmed that the presence of hAFSCs into scaffold created an inflammatory highly vascularized microenvironment driving neo-tissue formation into the construct. Moreover, the timing was critical for the type of response observed: after 1 week the histological samples were characterized by the presence of a high number of leucocytes, while at 4–8 weeks the presence of vessels and neo-formed heterogeneous tissues were predominant in the hAFSC-seeded scaffolds, but not in the empty scaffolds. Therefore, it appears that the implanted hAFSCs play a pivotal role in mounting an immediate inflammatory response that possibly mediates a subsequent recruitment of host's endothelial progenitors and other progenitor cells able to form tissues of mesodermal origin such as fat, muscle, fibrous tissue and immature bone. It is to note that in the same mouse model, scaffold seeded with human bone marrow derived MSCs remain into the scaffold, become osteoblasts and directly deposit bone tissue on the ceramic surface [45]. Therefore, it appears that only the more uncommitted hAFSCs would have migratory properties to wounds and tissue lesion sites and a chemoattractant capacity toward a wide spectrum of different cell types involved in tissue regeneration/repair processes. Interesting, mouse bone marrow derived MSCs, which are less committed than their human counterpart, were able to recruit cells migrating from the host to the MSC-seeded ceramic [11]. At late implantation times the only new tissue inside the scaffold pore was bone formed through an endochondral process [46]. It is tempting to speculate that the mouse bone marrow derived MSC maintain some “memory” of the tissue of origin and possibly contribute to the formation of a stem cell niche specifically promoting bone formation. On the contrary, hAFSCs can recruit endothelial and multipotent mesenchymal stem/progenitors, but do not have “memory” of a specific tissue and cannot contribute to the formation of a specific tissue stem cell niche. Therefore different types of mesenchymal tissues could be formed by the host recruited multipotent stem cells.

5. Conclusion

Here, we provided information about the stem characteristics and functional properties of the *in vitro* expanded hAFSCs at different culture stages and we showed *in vivo* behavior of hAFSCs in terms of: (i) recruitment of host progenitor cells, (ii) homing towards injured sites and (iii) multipotentiality in tissue repair. Indeed, these cells are a very appealing source of stem cells that may be useful for clinical application in regenerative medicine.

Acknowledgements

This work was supported by funds from European Community and from AIRC2009 to AP (IG8761). We thank the Galliera Genetic Bank - Network of Telethon Genetic Biobanks (project GTB07001) for providing us with a karyotyping service for characterization of cells.

References

- [1] Caplan AI. Mesenchymal stem cells. *J Orthop Res* 1991;9(5):641–50.
- [2] Roubelakis MG, Pappa KI, Bitsika V, Zagoura D, Vlahou A, Papadaki HA, et al. Molecular and proteomic characterization of human mesenchymal stem cells derived from amniotic fluid: comparison to bone marrow mesenchymal stem cells. *Stem Cells Dev* 2007;16(6):931–52.

- [3] Walther G, Gekas J, Bertrand OF. Amniotic stem cells for cellular cardiomyoplasty: promises and premises. *Catheter Cardiovasc Interv* 2009;73(7):917–24.
- [4] De Coppi P, Bartsch Jr G, Siddiqui MM, Xu T, Santos CC, Perin L, et al. Isolation of amniotic stem cell lines with potential for therapy. *Nat Biotechnol* 2007;25(1):100–6.
- [5] Pappa KI, Anagnostou NP. Novel sources of fetal stem cells: where do they fit on the developmental continuum? *Regen Med* 2009;4(3):423–33.
- [6] Marcus AJ, Coyne TM, Black IB, Woodbury D. Fate of amnion-derived stem cells transplanted to the fetal rat brain: migration, survival and differentiation. *J Cell Mol Med* 2008;12(4):1256–64.
- [7] Perin L, Sedrakyan S, Da Sacco S, De Filippo R. Characterization of human amniotic fluid stem cells and their pluripotential capability. *Methods Cell Biol* 2008;86:85–99.
- [8] Buoni S, Zannoli R, Macucci F, Pucci L, Mogni M, Pierluigi M, et al. Familial robertsonian 13;14 translocation with mental retardation and epilepsy. *J Child Neurol* 2006;21(6):531–3.
- [9] Prusa AR, Marton E, Rosner M, Bernaschek G, Hengstschlager M. Oct-4-expressing cells in human amniotic fluid: a new source for stem cell research? *Hum Reprod* 2003;18(7):1489–93.
- [10] Atala A. Recent developments in tissue engineering and regenerative medicine. *Curr Opin Pediatr* 2006;18(2):167–71.
- [11] Tasso R, Augello A, Boccardo S, Salvi S, Carida M, Postiglione F, et al. Recruitment of a host's osteoprogenitor cells using exogenous mesenchymal stem cells seeded on porous ceramic. *Tissue Eng Part A* 2009;15(8):2203–12.
- [12] Tasso R, Fais F, Reverberi D, Tortelli F, Cancedda R. The recruitment of two consecutive and different waves of host stem/progenitor cells during the development of tissue-engineered bone in a murine model. *Biomaterials* 2010;31(8):2121–9.
- [13] Kolambkar YM, Peister A, Soker S, Atala A, Gulberg RE. Chondrogenic differentiation of amniotic fluid-derived stem cells. *J Mol Histol* 2007;38(5):405–13.
- [14] Corselli M, Parodi A, Mogni M, Sessarego N, Kunkl A, Dagna-Bricarelli F, et al. Clinical scale ex vivo expansion of cord blood-derived outgrowth endothelial progenitor cells is associated with high incidence of karyotype aberrations. *Exp Hematol* 2008;36(3):340–9.
- [15] Moretta A, Poggi A, Pende D, Tripodi G, Orengo AM, Pella N, et al. CD69-mediated pathway of lymphocyte activation: anti-CD69 monoclonal antibodies trigger the cytolytic activity of different lymphoid effector cells with the exception of cytolytic T lymphocytes expressing T cell receptor alpha/beta. *J Exp Med* 1991;174(6):1393–8.
- [16] Musso A, Zocchi MR, Poggi A. Relevance of the mevalonate biosynthetic pathway in the regulation of bone marrow mesenchymal stromal cell-mediated effects on T cell proliferation and B cell survival. *Haematologica*; 2010 [Epub ahead of print].
- [17] Prevosto C, Zancolli M, Canevali P, Zocchi MR, Poggi A. Generation of CD4+ or CD8+ regulatory T cells upon mesenchymal stem cell-lymphocyte interaction. *Haematologica* 2007;92(7):881–8.
- [18] Martin I, Muraglia A, Campanile G, Cancedda R, Quarto R. Fibroblast growth factor-2 supports ex vivo expansion and maintenance of osteogenic precursors from human bone marrow. *Endocrinology* 1997;138(10):4456–62.
- [19] Sacchetti B, Funari A, Michienzi S, Di Cesare S, Piersanti S, Saggio I, et al. Self-renewing osteoprogenitors in bone marrow sinusoids can organize a hematopoietic microenvironment. *Cell* 2007;131(2):324–36.
- [20] Rittie L, Fisher GJ. Isolation and culture of skin fibroblasts. *Methods Mol Med* 2005;117:83–98.
- [21] Ellison D, Rigg J, McConnell SJ, Alexander AD, Yager RH. Use of antibiotics in the preparation of Canine kidney tissue culture Vaccines to Eliminate Leptospirosis. *Appl Microbiol* 1965;13:595–9.
- [22] Igarashi S. A simple enzymatic method for isolation of hepatocytes. *Experientia* 1977;33(10):1401–2.
- [23] Kruisbeek AM. Isolation of mouse mononuclear cells. *Curr Protoc Immunol*; 2001 [Chapter 3]:Unit 3.1.
- [24] Bianchi G, Banfi A, Mastrogiacomo M, Notaro R, Luzzatto L, Cancedda R, et al. Ex vivo enrichment of mesenchymal cell progenitors by fibroblast growth factor 2. *Exp Cell Res* 2003;287(1):98–105.
- [25] Rubio D, Garcia-Castro J, Martin MC, de la Fuente R, Cigudosa JC, Lloyd AC, et al. Spontaneous human adult stem cell transformation. *Cancer Res* 2005;65(8):3035–9.
- [26] Miura M, Miura Y, Padilla-Nash HM, Molinolo AA, Fu B, Patel V, et al. Accumulated chromosomal instability in murine bone marrow mesenchymal stem cells leads to malignant transformation. *Stem Cells* 2006;24(4):1095–103.
- [27] Sessarego N, Parodi A, Podesta M, Benvenuto F, Mogni M, Raviolo V, et al. Multipotent mesenchymal stromal cells from amniotic fluid: solid perspectives for clinical application. *Haematologica* 2008;93(3):339–46.
- [28] Katebi M, Soleimani M, Cronstein BN. Adenosine A2A receptors play an active role in mouse bone marrow-derived mesenchymal stem cell development. *J Leukoc Biol* 2009;85(3):438–44.
- [29] Eltzschig HK, Thompson LF, Karhausen J, Cotta RJ, Ibla JC, Robson SC, et al. Endogenous adenosine produced during hypoxia attenuates neutrophil accumulation: coordination by extracellular nucleotide metabolism. *Blood* 2004;104(13):3986–92.
- [30] Mariotti E, Mirabelli P, Abate G, Schiattarella M, Martinelli P, Fortunato G, et al. Comparative characteristics of mesenchymal stem cells from human bone marrow and placenta: CD10, CD49d, and CD56 make a difference. *Stem Cells Dev* 2008;17(6):1039–41.
- [31] Brooke G, Tong H, Levesque JP, Atkinson K. Molecular trafficking mechanisms of multipotent mesenchymal stem cells derived from human bone marrow and placenta. *Stem Cells Dev* 2008;17(5):929–40.
- [32] Nomura T, Ashihara E, Tateishi K, Ueyama T, Takahas-Hi T, Yamagishi M, et al. Therapeutic potential of stem/progenitor cells in human skeletal muscle for cardiovascular regeneration. *Curr Stem Cell Res Ther* 2007;2(4):293–300.
- [33] Moretta A, Olive D, Poggi A, Pantaleo G, Mawas C, Moretta L. Modulation of surface T11 molecules induced by monoclonal antibodies: analysis of the functional relationship between antigen-dependent and antigen-independent pathways of human T cell activation. *Eur J Immunol* 1986;16(11):1427–32.
- [34] Zanders ED, Lamb JR, Feldmann M, Green N, Beverley PC. Tolerance of T-cell clones is associated with membrane antigen changes. *Nature* 1983;303(5918):625–7.
- [35] Dugger K, Lowder TW, Tucker TA, Schwiebert LM. Epithelial cells as immune effector cells: the role of CD40. *Semin Immunol* 2009;21(5):289–92.
- [36] Rutishauser RL, Kaech SM. Generating diversity: transcriptional regulation of effector and memory CD8 T-cell differentiation. *Immunol Rev* 2010;235(1):219–33.
- [37] Nauta AJ, Fibbe WE. Immunomodulatory properties of mesenchymal stromal cells. *Blood* 2007;110(10):3499–506.
- [38] Matsumoto T, Mifune Y, Kawamoto A, Kuroda R, Shoji T, Iwasaki H, et al. Fracture induced mobilization and incorporation of bone marrow-derived endothelial progenitor cells for bone healing. *J Cell Physiol* 2008;215(1):234–42.
- [39] Revoltella RP, Papini S, Rosellini A, Michelini M, Franceschini V, Ciorba A, et al. Cochlear repair by transplantation of human cord blood CD133+ cells to nod-scid mice made deaf with kanamycin and noise. *Cell Transplant* 2008;17(6):665–78.
- [40] T.A. R. Thy-1 as a regulator of cell-cell and cell-matrix interactions in axon regeneration, apoptosis, adhesion, migration, cancer, and fibrosis. *FASEB J* 2006;20:1045–54.
- [41] Elices MJOL, Takada Y, Crouse C, Luhowskyj S, Hemler ME, Lobb RR. VCAM-1 on activated endothelium interacts with the leukocyte integrin VLA-4 at a site distinct from the VLA-4/fibronectin binding site. *Cell* 1990;60(4):577–84.
- [42] Perin L, Sedrakyan S, Giuliani S, Da Sacco S, Carraro G, Shiri L, et al. Protective effect of human amniotic fluid stem cells in an immunodeficient mouse model of acute tubular necrosis. *PLoS One* 2010;5(2):e9357.
- [43] De Coppi P, Allegari A, Chiavegato A, Gasparotto L, Piccoli M, Taiani J, et al. Amniotic fluid and bone marrow derived mesenchymal stem cells can be converted to smooth muscle cells in the cryo-injured rat bladder and prevent compensatory hypertrophy of surviving smooth muscle cells. *J Urol* 2007;177(1):369–76.
- [44] Yoon BS, Moon JH, Jun EK, Kim J, Maeng I, Kim JS, et al. Secretory profiles and wound healing effects of human amniotic fluid-derived mesenchymal stem cells. *Stem Cells Dev* 2010;19(6):887–902.
- [45] Muraglia A, Martin I, Cancedda R, Quarto R. A nude mouse model for human bone formation in unloaded conditions. *Bone* 1998;22(5 Suppl):131S–4S.
- [46] Tortelli F, Tasso R, Loiacono F, Cancedda R. The development of tissue-engineered bone of different origin through endochondral and intramembranous ossification following the implantation of mesenchymal stem cells and osteoblasts in a murine model. *Biomaterials* 2010;31(2):242–9.